NMR Study of Gels of Isotactic Polystyrene and *cis*- or *trans*-Decalin

E. Pérez,† D. L. VanderHart,* and G. B. McKenna

Polymers Division, National Bureau of Standards, Gaithersburg, Maryland 20899.
Received November 20, 1987

ABSTRACT: Samples consisting of a high molecular weight ($M_w = 1.4 \times 10^6$) isotactic polystyrene (iPS) mixed, 25% by weight, with *cis*- or *trans*-decalin have been investigated by proton and ^{13}C NMR. The most studied samples were gels formed by quenching the solutions to 253 K, although some data on gels formed at 296 K are also reported. Comparison is further made with samples crystallized at 347 K. Most of the NMR data were obtained on nonspinning samples, although magic angle spinning was attempted on one gel sample. Variable-temperature proton spectra covered the range from solvent freezing to gel melting temperatures. The principal motivation was to investigate the nature of the iPS-rich phase in the gels since previous studies have claimed evidence either for a crystal structure different from the usual 3_1 helix or for a polymer/solvent complex. The existence of a polymer/solvent complex (or a solvated crystal structure) was shown to be unlikely on the basis of the NMR findings of high solvent mobilities and widely disperse segment mobilities for iPS. NMR results on the solvent freezing behavior support earlier DSC findings, i.e., sizeable fractions of solvent molecules undergo a gradual immobilization as temperature is lowered compared with the rapid freezing behavior of the pure solvent. In the absence of a polymer/solvent complex, the alternate explanation offered for the gradual freezing is that uncondensed iPS chain segments partition space into a distribution of cavity sizes, which, in turn, impose on the solvent a size-dependent depression of solvent freezing points and enthalpies. Above the solvent freezing temperatures, proton spectra were analyzed in terms of a broad, glasslike and a narrow, liquidlike signal. As the temperature is raised from the solvent freezing point, the broad signal weakens and narrows slightly; correspondingly, the liquidlike signal grows. The thermal reversibility of the line shapes was investigated and established between the solvent freezing points and 296 K. This continuous change and the reversibility offer insight into the growth process of the rigid iPS phase. Whether the structure of the rigid PS segments in the gel is ordered or disordered remains a largely unanswered question. Evidence for disorder is a faster proton dipolar relaxation time and a reduced line width at 296 K compared to either the glassy state or the 3_1 helical crystalline state. Evidence for order is that the aliphatic and the unprotonated aromatic carbon resonances in the CP-MAS spectrum at 296 K have intermediate line widths and a unique chemical shift difference compared to the corresponding parameters in glassy (disordered) and crystalline (ordered) 3_1 helical preparations. Also, the energetics of condensation favor the ordered over the disordered structures. It is concluded that the rigid portion of the gel probably has more order than the glass, but more disorder than the 3_1 helical crystal. Finally, it is shown that the NMR behavior of the gel is very different from that of a preparation of solution-crystallized iPS.

Introduction

There has been considerable interest recently in the behavior of synthetic polymer gels formed by an appropriate thermal history either from crystallizable or noncrystallizable polymer solutions.[1-16] In this study we will address the isotactic polystyrene (iPS) system which has been found to be interesting for several reasons. First, the gels themselves, which are formed by a quench to below the Θ temperature of the solvent, seemed to exhibit a new "crystal" structure for iPS.[1] This structure was interpreted to be a 12_1 helix,[13,15] in contrast to the normal 3_1 helix[17] for iPS. Further, it was assumed[1] that the gel is a classical fringed micellar type with the new "crystal" form acting as cross-linking points for swollen "rubbery" chains. On the other hand, Guenet[8] found that the chain conformation in the new "crystalline" form may not be a 12_1 helix and, in neutron scattering studies on the pure decalin solvent as well as the gel, demonstrated that the peak, attributed to the 0.51-nm spacing of the 12_1 helix, persists when only solvent is present. He also proposed,[8] on the basis of DSC results, that the gel structure is made up of solvated crystals of iPS. Furthermore, in morphological studies of transformed gels whose crystalline regions possessed the 3_1 helical structure, Guenet et al.[7] found that the transformed gel exhibited a texture with a characteristic spacing of several tenths of a micrometer, i.e., distances of the order of the contour length, yet much greater than the radius of gyration, for their polymer chain.

In recent work Guenet and McKenna[10] have reported that in iPS–*cis*-decalin (iPS–*c*-D) gels the concentration dependence of the compression modulus does not follow a power law; rather, the modulus curve is approximately concave with evidence of rapid changes over certain narrow concentration ranges. Such behavior is not consistent with that observed[18] classically for other gels, e.g., poly(vinyl chloride), which have been interpreted as having a fringed micellar structure.[19]

A somewhat different interpretation of gel structure is offered by Domszy et al.[5] In different ethylenic polymers and copolymers they found a continuity of thermodynamic and structural properties between crystallites formed in dilute solution and in the gels. They also show that the general form of the gelation time versus temperature plot for iPS in *trans*-decalin is parallel to that of the ethylenic polymers. Therefore, they reject the fringed micelle model for the gels and consider gel formation to be an extension of chain-folded crystallization from dilute solution. Upon increasing polymer concentration, there is a concentration at which the probability becomes significant that a given chain will participate in more than one region of crystallization. This, in their view, represents the onset of gel formation.

The purpose of this study was to use proton and ^{13}C NMR techniques to study gels of iPS in *cis*- and *trans*-decalin, with a view toward providing information about the mobility of both the polymer and the solvent in the gel state. Such information should aid in discriminating

† Present address: Instituto de Plasticos y Caucho, Juan de la Cierva 3, 28006-Madrid, Spain.

0024-9297/88/2221-2418$01.50/0

between the models of gel structure which have been proposed.

Experimental Section

Materials and Gel Preparation. The iPS used for this study was the same as the "F3B" sample described in an earlier publication.[10] This polymer has a percentage of isotactic diads exceeding 96% as determined by solution NMR. M_w is 1.44×10^6 and the polydispersity is 2.0. The *cis*- and *trans*-decalin solvents were supplied by Aldrich Chemical and were used without further purification.

Gels having 24–25% iPS by weight were prepared by weighing the components, sealing them under vacuum into glass NMR tubes having either 5- or 8-mm o.d.'s, heating them at 454 K until the solutions were homogeneous, and transferring the tubes rapidly to a liquid bath at the desired temperature. The total volume of the tubes was usually about twice that of the polymer solutions. In the quenching of the hot solutions, the tubes were immersed initially only to the meniscus of the solution in order to avoid the flashing of the solvent out of the solution onto cold walls above the solution. After the short initial cooldown, the whole tube was immersed. The quench temperature for the formation of the gels was 253 K unless otherwise noted.

Only one sample, iPS in *trans*-decalin (iPS–*t*-D), was prepared for ^{13}C magic angle spinning[20-23] (MAS). This sample was prepared in a sealed glass tube of the same i.d. as the NMR rotor (6 mm). After the gel was made, the tube was broken open and the sample was transferred to a machinable ceramic rotor which was designed for spinning liquid samples and had a closure on only one end.

Two samples of pure iPS were also studied. One was the as-precipitated (at 35 °C from a 1% toluene solution using ethanol) and dried F3B sample,[10] and the other was made from the first by annealing at 453 K for 24 h under vacuum.

NMR Spectrometer and Techniques. The spectrometer is a Bruker CXP200[24] operating at a magnetic field of 4.7 T. Three probes were used: a nonspinning 5-mm low-Q proton probe, a nonspinning 8-mm high-Q probe which is doubly tuned for ^{13}C and ^1H irradiation and observation, and a 7-mm high-Q MAS probe also doubly tuned for ^{13}C and ^1H irradiation and observation. The sample tube axis is horizontal in both nonspinning probes.

The pulse programs employed were of the following types: simple one-pulse/observe (Bloch decay), cross polarization[25] (CP), or $90°_x$–τ–$45°_y$–t–$45°_{x,y,-x,y}$–observe[26] (T_{1D}). The indicated phase cycling, ($x = 0°$, $y = 90°$, $-x = 180°$, and $-y = 270°$) of the latter 45° pulse in the T_{1D} sequence was used to suppress unwanted signals. For observation of the broad PS line in proton spectra, the maximum dwell time was 4 μs with a 4-μs delay before acquisition. When proton spectra of the gels were acquired by using the 8-mm probe, receiver saturation was avoided by attenuating the proton radiofrequency (rf) level, reducing the pulse width to 1 μs, and detuning the probe. The rf levels used for CP corresponded to rotating frequencies of 65–70 kHz. CP times were in the range 0.7–1.0 ms.

Measurement of temperature in the variable-temperature experiments was accomplished by using a thermocouple placed about 1 mm above the coil. Uncertainties in sample temperature are limited to ±3 K. Actual sample temperatures were also measured by using a methanol sample[27] in a calibration run.

DSC. Differential scanning calorimetry measurements were performed on a small piece of the iPS–*t*-D sample left over after the rotor was filled for the CP-MAS experiment. This DSC sample was stored in the freezer in a sealed tube for 2 weeks prior to the DSC run. The calorimeter was a Perkin-Elmer DSC-2[24] equipped with a refrigeration unit for low-temperature operation. Scan rates were 10 K/min for all scans. In a cooling run, this controlled rate could only be maintained down to 211 K. Further cooling occurred at a slower pace. The low temperature achieved prior to the heating run was 190 K.

Results

^{13}C Nonspinning Spectra. An important area which NMR measurements can address is how gel formation affects the mobility of the iPS chains and the solvent molecules. Several experiments on iPS gels using both *cis*- and *trans*-decalin were performed. Figure 1 compares a nonspinning ^{13}C CP spectrum of an iPS–*t*-D gel formed at 253 K with that of the glassy, as-precipitated polymer. Also shown is a difference spectrum. It is evident that in the gel there is a portion of polymer which possesses a rigidity comparable to that of the glassy polymer, judging by the similarity in the chemical shift anisotropy patterns of the aromatic carbons. These anisotropy patterns are most evident in the 80–230 ppm range although the upfield edge of these lines overlaps the aliphatic region (10–70 ppm).[28] A 22% rigid fraction of iPS segments is estimated in the iPS–*t*-D gel from the known weights of iPS in the two samples assuming the same cross-polarization efficiencies for the iPS carbons in the glassy state and in the gel.

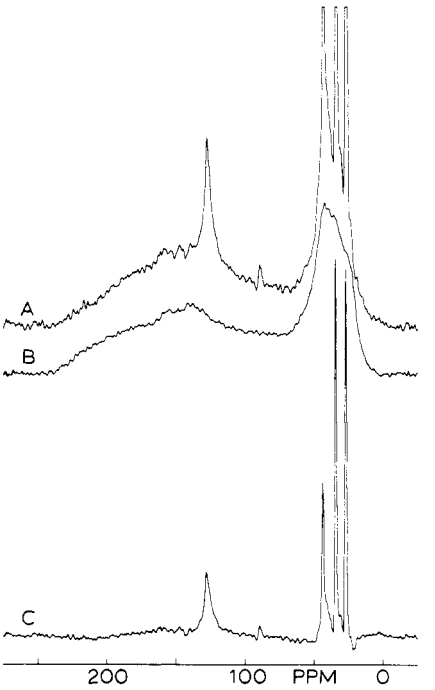

Figure 1. ^{13}C nonspinning CP spectra, 50.3 MHz, at 296 K; CP time is 0.7 ms: (A) 25% by weight iPS in *trans*-decalin (iPS–*t*-D), gel formed at 253 K; (B) glassy iPS; (C) difference spectrum, 0.5(A – B). Spectrum B is normalized to match the intensity of the downfield resonance of the gel. A 20-Hz Lorentzian line broadening is present. The sharp lines in the 25–50 ppm region belong to the solvent; the sharper feature at about 128 ppm corresponds to mobile protonated aromatic PS carbons. The weak feature at about 90 ppm is spurious; this is the position of the rf carrier. Lack of broader intensities in the aliphatic region (10–70 ppm) in spectrum C indicates that there are no solvent molecules immobilized in the PS matrix.

Figure 1 also displays narrow resonances which one can associate with both the iPS and decalin carbons. Narrow resonances in a nonspinning sample imply nearly isotropic mobility, fast on a timescale (30–100 μs) of the inverse chemical shift anisotropy width. The presence of fast isotropic mobility along with translational mobility also reduces the carbon–proton dipolar interactions which are necessary for CP. In the limit of liquidlike mobility, the only available CP mechanism[29,30] is the scalar C–H coupling, which mechanism is very inefficient under these experimental conditions. It follows that the true ratio of broad to narrow resonances in the gel is very much smaller than appears in the gel spectrum of Figure 1. The narrow PS resonance in this spectrum indicates that both rigid and mobile segments coexist on a 100-μs time scale. On the other hand, the level of CP signal generated by the solvent carbons is about 14 times larger than was obtained from the same amount of pure solvent, although this signal

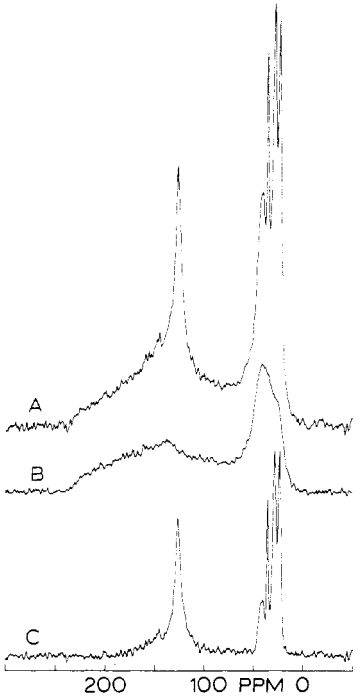

Figure 2. As in Figure 1 except (A) corresponds to the gel having 25% by weight iPS in *cis*-decalin (iPS–*c*-D).

is only about 1% of that expected if all the solvent molecules are rigid. To argue on this basis that the PS molecules impose some restriction on the isotropic character of motion is speculative because the CP intensity in a liquid under these conditions is very sensitive to the exact rf matching conditions.[29,30] While the matching conditions are monitored closely, we do not have a good idea about intensity reproducibility on a pure liquid sample.

From the point of view of the gel possibly possessing a crystal structure that incorporates solvent, we find it significant that there is no spectral evidence for rigid, or even anisotropically mobile, solvent molecules. Relatively rigid decalin molecules, fixed in a crystal lattice, should produce resonances having chemical shift anisotropy patterns which are 10–50 ppm in width and lie in the 10–70 ppm range. The difference spectrum, Figure 1C, indicates that the broad resonances which appear in this range can be explained by the aliphatic carbon resonances of the iPS which are associated with the rigid aromatic segments. In principle, a very short proton rotating frame relaxation time, $T_{1\rho}^{H}$, or a very short carbon transverse relaxation time, T_2^C, could also account for missing CP signals from PS-complexed solvent molecules. Neither of these situations appears likely, however, because the intrinsic $T_{1\rho}^{H}$ and T_2^C for any strongly bound decalin molecules should be highly correlated as is found in poly(ethylene oxide).[31] At the same time, in a strong complex, the $T_{1\rho}^{H}$ of the decalin and the solidlike iPS segments should be very close as a result of spin exchange. In contradiction to this reasoning, it is seen that the $T_{1\rho}^{H}$ for the more rigid iPS segments is sufficiently long to cross polarize the corresponding iPS carbons. Thus, from this carbon spectrum and the foregoing argument, we conclude that if any solvent complex exists, the orientation and position of the solvent molecules is transient on a time scale shorter than 1 μs.

Similar CP results are shown in Figure 2 for an iPS–*c*-D gel sample under the same conditions as those in Figure 1. The principal differences, relative to Figure 1, are that the intensity of the liquidlike line at 128 ppm is about 3 times stronger and there seems to be a larger fraction of

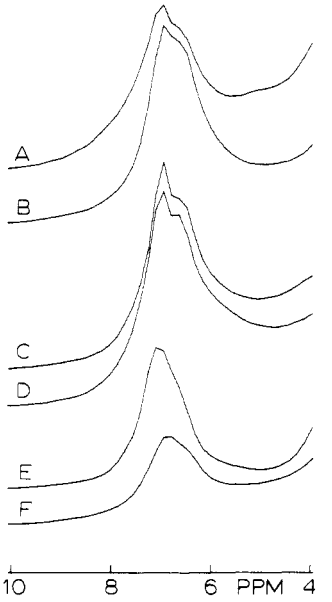

Figure 3. Region of narrowed proton aromatic PS resonances at 200 MHz and 296 K for different preparations. All spectra have been normalized to the same total intensity, including the broad resonances. (A) iPS–*c*-D, gel formed at 253 K; (B) iPS–*t*-D, gel formed at 253 K; (C) iPS–*c*-D, gel formed at 296 K; (D) iPS–*t*-D, gel formed at 296 K; (E) iPS–*c*-D, crystallized for 120 h at 347 K; (F) iPS–*t*-D, crystallized for 16 h at 347 K. The base line on the upfield side rises because of the strong upfield aliphatic resonance originating from the aliphatic proton resonances of the solvent and the iPS. Crystallization of the iPS causes a reduction in the fraction of mobile iPS segments. This effect is more pronounced in the iPS–*t*-D sample which crystallizes faster than the iPS–*c*-D sample.

PS with intermediate mobility according to the difference spectrum, Figure 2C. Again it is risky to place a lot of significance on the stronger CP intensity of the liquidlike line, since the CP behavior of liquidlike resonances is so strongly dependent on the exact matching conditions.[29,30] The reason for the greater fraction of chains with intermediate mobility is not clear. In spite of the broader base for the aliphatic resonances in Figure 2C compared with Figure 1C, this broader base can be accounted for by the expected aliphatic carbon resonances of PS corresponding to the more intense intermediate-line-width component in the aromatic region of Figure 2C. Thus, the broader base of the aliphatic region in Figure 2C compared with that of Figure 1C does not imply any notable contribution from strongly complexed solvent molecules in the polymer matrix.

Proton Nonspinning Spectra. 1. Spectra at Ambient Temperature. The Bloch-decay proton spectra of either iPS–*t*-D or iPS–*c*-D gels consist of narrow and broad contributions, consistent with the ^{13}C CP results. These proton spectra are undistorted because care was taken to ensure equilibrium of all proton spin populations. The narrow portion of the line has high-resolution attributes, i.e., the aliphatic resonances of the very mobile PS protons and the solvent protons are found in the 0–3 ppm range while the much weaker aromatic proton resonance for the mobile PS segments are found near 7 ppm. Figure 3 shows only the latter region of the proton spectra, taken at ambient temperature, for three preparations of the two kinds of 25% iPS/75% decalin systems. The spectra in Figure 3A,C,E correspond to the iPS–*c*-D system and the spectra in Figure 3B,D,F represent the iPS–*t*-D system. Taken in pairs, these spectra respectively derive from preparations with quenching temperatures of 253, 296, and 347 K. The spectra in Figure 3A–D represent gels while the

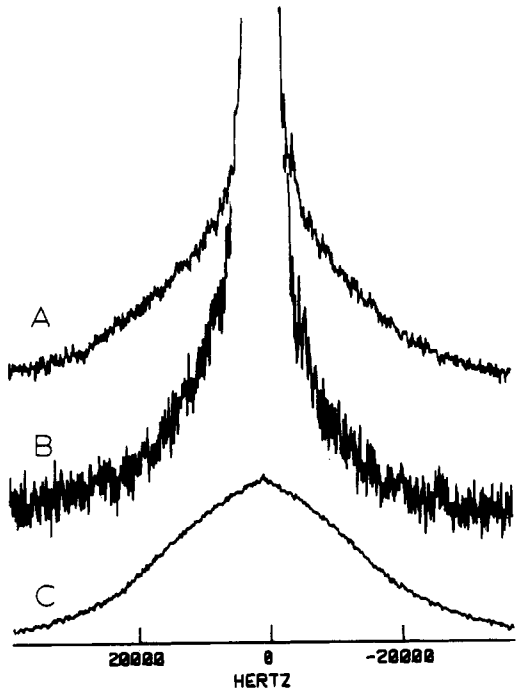

Figure 4. Broad portions of proton spectra at 296 K for different preparations of the iPS–*t*-D sample: (A) crystallized at 347 K for 16 h; (B) gel formed at 253 K; (C) glassy iPS. (C) glassy iPS. (B) has a total integral twice that of (A) in this plot.

spectra in Figure 3E,F correspond to a preparation containing solution-grown crystals.[1] In plotting each spectrum in Figure 3, the total proton intensities were first normalized to the same areas; therefore, the intensities shown represent relative fractions of highly mobile PS residues. For the gels, this fraction is about the same for the two solvents and quench temperatures. On the other hand, there is a substantial difference between the iPS–*c*-D and iPS–*t*-D systems crystallized at a temperature of 347 K. The fraction of mobile PS segments is much higher in the iPS–*c*-D sample in spite of the fact that this sample was crystallized for 120 h in contrast to 16 h for the iPS–*t*-D sample. The most likely source of this difference is the apparently more sluggish crystallization kinetics in *cis*-decalin versus *trans*-decalin, i.e., the *trans*-decalin sample turned white after 2 h, whereas the *cis*-decalin sample took 24 h to become cloudy.

The broad counterpart resonances associated with the more rigid PS segments and any possible solvating decalin molecules are illustrated in the 296 K spectra of Figure 4. A spectral width 83 times that of Figure 3 is used, and the spectra are also more amplified. The intense, narrow resonances are truncated. Spectrum 4A is that of the iPS–*t*-D prepared at 347 K; spectrum B is the same sample redissolved at 454 K and gelled at 253 K. For comparison, the spectrum in Figure 4C is that of the as-precipitated glassy iPS. The difference in the intensity of the broad components in spectra A and B of Figure 4 is consistent with the presence of the solution-grown crystals in the 347 K preparation and is qualitatively consistent with the weaker resonance of spectrum F compared to B of Figure 3. The broad gel resonance in spectrum B, Figure 4, is, on average, narrower than the broad resonances of spectra A and C of Figure 4, although the weak wings of the resonances in all three spectra extend comparably far. This somewhat narrower gel resonance does not necessarily imply that those segments in the *interior* of the condensed regions of the gel have higher mobilities than, say, the glass; the coexistence of liquidlike and condensed iPS segments implies an interface with intermediate mobility. The line

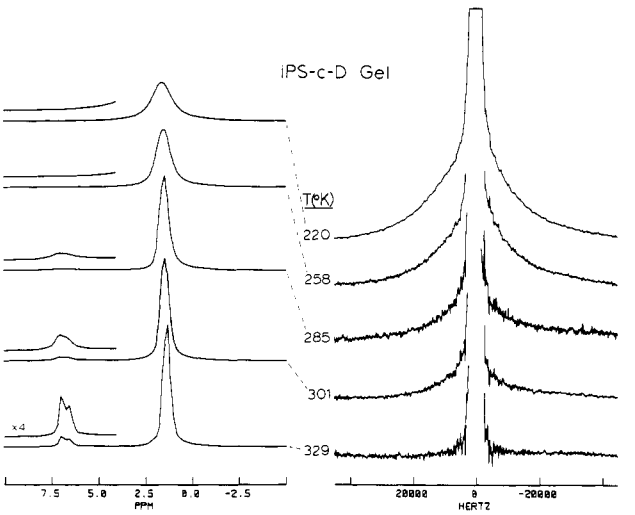

Figure 5. Selected 200-MHz proton spectra, taken at various temperatures, of the iPS–*c*-D gel formed at 253 K. Two spectral displays are given, the narrow central region on the left and the broad, vertically amplified spectra on the right. On the left, the region of mobile aromatic PS resonances is also vertically amplified (×4). Temperatures for this cooling cycle are indicated and all spectra in each set are normalized to the same total intensity. Intensity growth in the broad base is accompanied by decay in the narrow aromatic PS signals at 7 ppm.

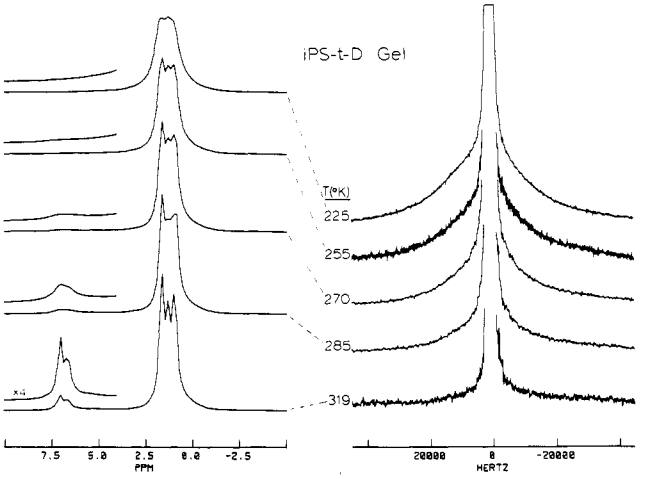

Figure 6. Selected proton spectra, taken at various temperatures, for the iPS–*t*-D gel formed at 253 K. The format is that of Figure 5.

shape of the base of the gel resonance and its interpretation depend on the fraction of interface protons, which, in turn, is strongly dependent on the surface-to-volume ratio. We shall return to this point in connection with the variable-temperature experiments.

2. Variable-Temperature Spectra above the Solvent Freezing Temperature. Nonspinning proton spectra of the iPS–*t*-D and iPS–*c*-D gels formed at 253 K were taken at various temperatures. The spectral changes with temperature could yield information about whether the rigid regions of the PS in the gels correspond to crystals of any kind. If these regions are crystalline in a conventional sense, then they should exhibit a well-defined melting point. Moreover, there should be a range of temperature where the fraction of rigid material would not be a strong function of temperature.

Variable-temperature runs were conducted in two stages; first, temperature was cycled from room temperature to low temperature and back again. The second stage was a single run from room temperature to high temperature. Gels were freshly prepared before each run. Figures 5 and

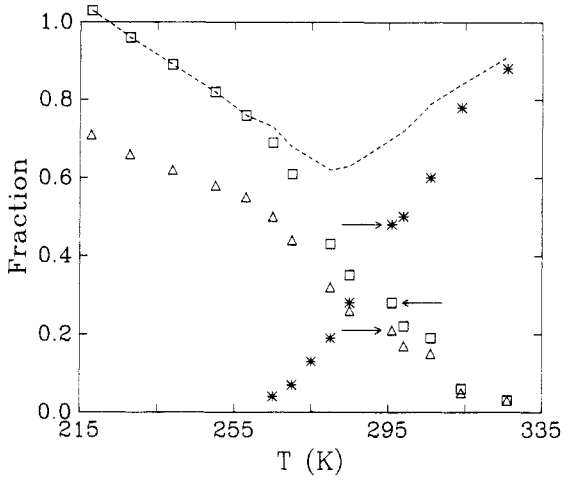

Figure 7. Temperature-dependent broad and narrow PS fractions deduced from the proton spectra, including those of Figure 5, for the iPS–*c*-D gel formed at 253 K. See text for definitions of the fractions and other details. (△) Broad fraction possessing the line width of glassy iPS; (□) "relatively rigid" fraction (see Figure 10); (*) narrow fraction; (---) sum of relatively rigid and narrow fractions. The three points denoted by arrows correspond to a gel formed by slowly cooling a solution from 304 to 295 K overnight in a Dewar. Uncertainties are ±0.06.

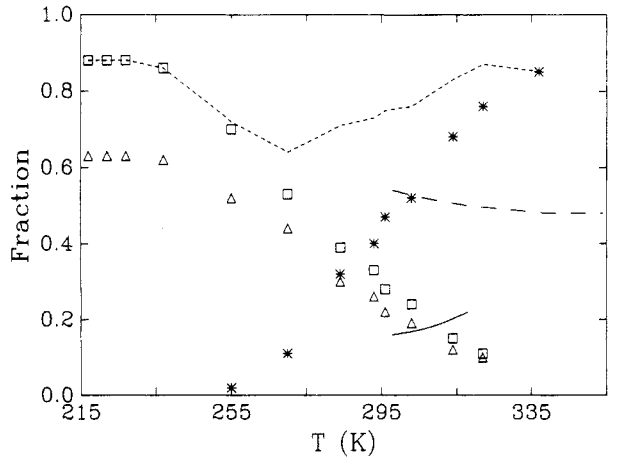

Figure 8. Temperature-dependent broad and narrow PS fractions deduced from the proton spectra, including those of Figure 6, for the iPS–*t*-D gel formed at 253 K. See the text and Figure 7 for other details. (△) Broad fraction possessing the line width of glassy iPS; (□) "relatively rigid" fraction (see Figure 10); (*) narrow fraction; (---) sum of the relatively rigid and the narrow fractions. The longer dashed line and the solid line are, respectively, relatively rigid and narrow fractions in a warming cycle for the iPS–*t*-D sample crystallized at 347 K for 16 h. Uncertainties are ±0.06.

6 show spectra obtained in cooling cycles at five selected temperatures above solvent freezing for the iPS–*c*-D and the iPS–*t*-D gels, respectively. In Figures 5 and 6 two spectral displays are given for each temperature, the high-resolution central portion and the broad spectral display with a large vertical amplification. Both gels show similar behavior. As the temperature decreases, the intensity of the broad resonance increases and that of the narrow PS resonance at 7 ppm decreases. The strong solvent line gets somewhat wider at the lower temperatures. This broadening is more pronounced in the iPS–*c*-D compared to the iPS–*t*-D gel. This line broadening probably corresponds to a true line width increase. At the same time, there could also be a temperature-dependent degradation of the magnetic field homogeneity since no attempt was made to retune the homogeneity of the magnetic field at each temperature. The better apparent resolution in the solvent line of the iPS–*t*-D gel relative

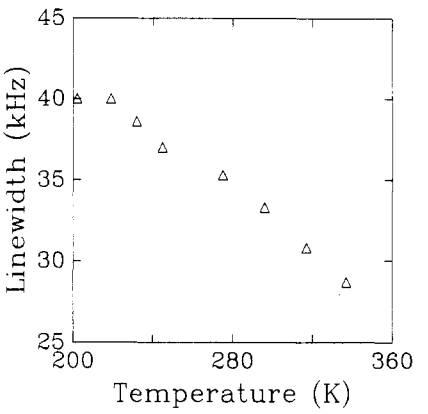

Figure 9. Proton full widths at half-height for glassy iPS as a function of temperature.

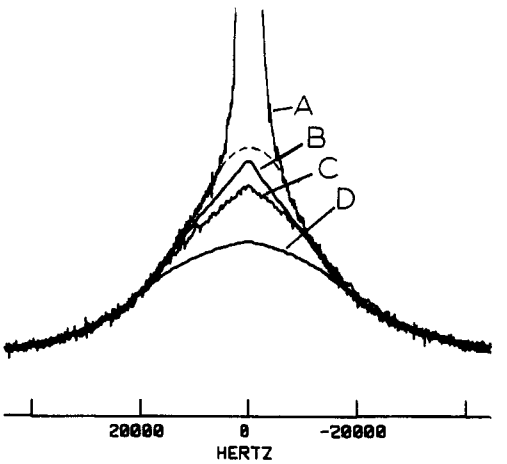

Figure 10. Proton line-shape comparison: (A) iPS–*t*-D gel, 225 K; (B) glassy iPS, 329 K; (C) glassy iPS, 296 K; (D) glassy iPS, 202 K. All spectra are normalized so that the intensities in the broad wings match. The dashed line drawn in (A) defines the intensity included in the "relatively rigid" component in Figures 7 and 8.

to the iPS–*c*-D gel is a result of the greater chemical shift dispersion of *trans*- versus *cis*-decalin.

The variable-temperature spectra of Figures 5 and 6 were analyzed in terms of their broad and narrow resonance contributions. These results are displayed in Figures 7 and 8 for the iPS–*c*-D and iPS–*t*-D gels, respectively. The narrow fraction is defined as the fractional intensity, relative to the intensity of the total spectrum, of the narrow aromatic PS line near 7 ppm divided by the known fraction of aromatic protons in the sample. The broad resonance fraction is defined in two ways in Figures 7 and 8. Each triangular symbol corresponds to that fraction of intensity in the broad base, which, at the given temperature, possesses a line shape like that of pure glassy iPS, divided by the known fraction of PS protons in the sample. Each square symbol corresponds to the "relatively rigid" fraction, i.e., those protons whose line widths exceed about 15 kHz, and is substantially broader than the solvent line width. Each point is again normalized against the known fraction of iPS protons. The reason that the broad component is analyzed in two different ways is that not all monomer units are expected to exist in ideal liquidlike or solidlike environments. Thus, the foregoing characterization of the broad fractions assumes that a heterogeneity of mobility (and line widths) exists from site to site and that the broad base does not represent the line shape for each and every constrained iPS proton.

The dependence of line width on temperature for glassy iPS is given in Figure 9 and an indication of the change

of line shape with temperature in the glass is given in Figure 10. Figure 10 illustrates these line shape changes in the context of comparing the broad resonance base of a low-temperature iPS–*t*-D gel with glassy iPS line shapes at various temperatures. Figure 9 shows that in the glass there is a definite change with temperature in the full width at half-height of the resonance. However, Figure 10 illustrates that this change in line width does not preserve the overall shape. Rather, as temperature increases, the line shape becomes less Gaussian, developing a more triangular-shaped profile. Meanwhile, the total width of the glassy spectra and the shape in the far wings are not noticeably temperature dependent. The stability of the shape in the wings of the spectrum is qualitatively consistent with the smaller amplitude molecular motions of the backbone protons below T_g.[32-35] The development of the more triangular-shaped central resonance at higher temperatures is consistent with the larger,[32,34] and inhomogeneously distributed,[35] amplitudes of motions associated with the aromatic protons[32,34,35] whose rigid lattice line width is considerably narrower than for the backbone protons.

Figure 10 offers insight into the interpretation of Figures 7 and 8. According to Figure 10, the analysis of the broad base of the proton resonance for the gel at 225 K would yield a broad fraction of 0.63, 0.71, or 0.77 depending on whether a glassy line shape corresponding to 202, 296, or 329 K, respectively, was used. The triangular data point in Figure 8 at 225 K corresponds to an analysis of spectrum A in Figure 10 using a line shape very similar to Figure 10D, while the square point in Figure 8 at 225 K represents the integral of the base of spectrum A, Figure 10, with its upper portion defined by the dashed line. It is clear from Figure 10 why, particularly at lower temperatures, the square points give much larger fractions than the triangular points in Figures 7 and 8.

According to Figures 7 and 8 the behavior of both gel systems is very similar, although the maximum rates of change with temperature of the narrow and broad resonances are slightly higher in the iPS–*c*-D gel compared to the iPS–*t*-D gel. At room temperature about 25–30% of the iPS segments are relatively rigid (square symbols) and 17–22% are rigid in the glass-like sense (triangular symbols) in both gels. These percentages are in reasonable agreement with the 22% estimated from the ^{13}C CP results in the iPS–*t*-D gel.

At low temperatures in Figures 7 and 8 the relatively rigid fractions range from 0.87 to 1.03 and the glasslike fractions range from 0.63 to 0.71 for iPS–*t*-D and iPS–*c*-D gels, respectively. The magnitude of the relatively rigid fraction and the stability of the line shape from 215 to 235 K in the iPS–*t*-D gel (see Figure 8) strongly suggest that the broad fraction arises entirely from iPS protons and that most of the iPS residues at these low temperatures exist in very constrained environments. In contrast, in the iPS–*c*-D gels at lower temperatures, the rigid fraction (see Figure 7) is not constant; moreover, fractions having widths in excess of 15 kHz increase also as the temperature is lowered. Therefore, while the fractions of the total intensities with line widths in excess of 15 kHz correspond reasonably well to the total number of iPS protons, we are less confident that no *cis*-decalin protons are contributing to this broader line width at low temperatures.

Another observation based on Figures 7 and 8 is that, over the temperature intervals investigated, the sums (dashed lines) of the relatively rigid and narrow fractions are often substantially less than unity; the sums reach a minimum of about 0.6 when the relatively rigid fractions are approximately 0.5. On the other hand, the sums are close to unity in the high-temperature region. The cause of the missing intensity is, to some extent, an underestimation in the integration of the narrow PS peak at lower temperatures because the apparent base line is rising due to the broadening of this PS resonance and a stronger overlapping with the solvent resonance. Nevertheless, it is clear that the principal explanation for the missing intensity is that the sum, as we have defined it, does not include protons with line widths in the range of about 400–15000 Hz. A chain segment, presumably fixed at both ends, will have an increasingly difficult time reorienting isotropically as the temperature is lowered if more residues condense and the portion remaining becomes more stretched out. We will return to this point in discussing gel structure.

Figures 7 and 8 also fail to reveal a sharp melting point which can be identified with a major portion of the iPS segments. If, for comparison, we consider a semicrystalline polymer like linear polyethylene (LPE) in the temperature range where the noncrystalline chains are above their glass transition temperature, the fractional intensity of the broad (crystalline) component of the proton spectrum remains about constant over a substantial range of temperature.[36] For a melt-crystallized sample, the fractional intensity begins to change perceptibly at temperatures about 75 K below the sample melting temperature, in reasonable analogy to the melting ranges for these gels. However, the range of temperatures over which this "melting" occurs in LPE is very dependent on sample preparation. Single-crystal preparations as well as extended-chain crystals have a much sharper melting behavior.[37] In that sense, the gel melting is more analogous to the melting of a rapidly crystallized LPE, rather than the melting of solution-grown crystals. By the time the originally reported[7] gel melting points (for 5% gels with iPS having $M_w = 2 \times 10^5$) are reached, i.e., 313 K for the iPS–*c*-D and 343 K for the iPS–*t*-D gels, the broad fractions are well below 0.1. A more recent study[38] recognized, partly in light of these NMR results, that melting in DSC is evidenced over ranges of temperature, i.e., 320–360 K for iPS–*t*-D gels and 305–340 K for iPS–*c*-D gels. Figures 7 and 8 indicate that less than 20% of the relatively rigid segments dissolve even in these temperature ranges.

The data below 296 K in Figures 7 and 8 pertain to spectra taken in cooling cycles. A few spectra were also taken during the warming cycle back to ambient temperature. Within experimental error, no hysteresis was indicated. At higher temperature, hysteresis cannot be tested with confidence since questions arise as to the aging of the gels. Also, the shape of the gel samples begins to change irreversibly near the reported[7] gel melting temperatures since our sample tubes are horizontal and any flow of the gel can transport some material outside of the NMR detection coil.

In summary, for Figures 5–8, no sharp melting of a fixed rigid (crystalline) fraction is observed at higher temperatures. Upon decreasing the temperature below ambient, iPS chains, still surrounded by solvent, progressively lose more reorientational freedom. At the same time, more segments are incorporated into a structure whose chains are quite rigid. The broad wings in the gel spectrum, just above the solvent freezing temperatures, indicate that a major portion of the backbone protons find themselves in an environment with rigidity comparable to the glass. At no temperature is there evidence for solvent molecules which experience any significant degree of immobilization as a result of the rigidifying of the PS chains. With respect

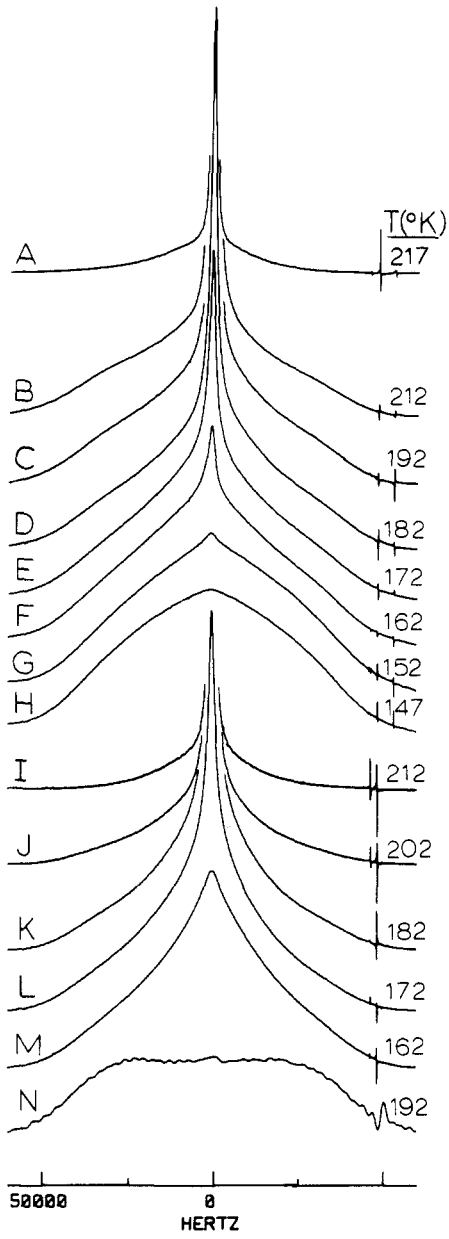

Figure 11. Broader portions of proton spectra below the solvent freezing temperatures (T_m = 230 and 243 K respectively for neat *cis*- and *trans*-decalin). Spectra are obtained in a cooling cycle so undercooling effects are present; temperatures are indicated. All spectra are normalized to the same total intensity. (A–H) iPS–*t*-D gel; (I–M) iPS–*c*-D gel; (N) pure frozen *cis*-decalin. Frozen *trans*-decalin produces a spectrum just like (N). Sharp features near 50 kHz are spurious.

to possible solvent incorporation within any organized PS structure, minor amounts of solvent with intermediate mobility will not be detected easily by using this proton line-shape analysis. The absence of broader solvent resonances in the ^{13}C CP spectra discussed earlier is a stronger indication that this kind of solvent molecule is absent, at least at 296 K.

3. Proton Spectra in the Region of Solvent Freezing. Since the lack of a full solvent melting endotherm in DSC measurements was one of the principal reasons for postulating a solvent/polymer complex,[7] we decided to investigate the proton spectra of the gels in the solvent freezing range. Figure 11 shows the broad components of these low-temperature line shapes, where each line shape has been normalized to the same total intensity. Spectra A–H of Figure 11 correspond to the iPS–*t*-D gel, spectra I–M correspond to the iPS–*c*-D gel at the temperatures

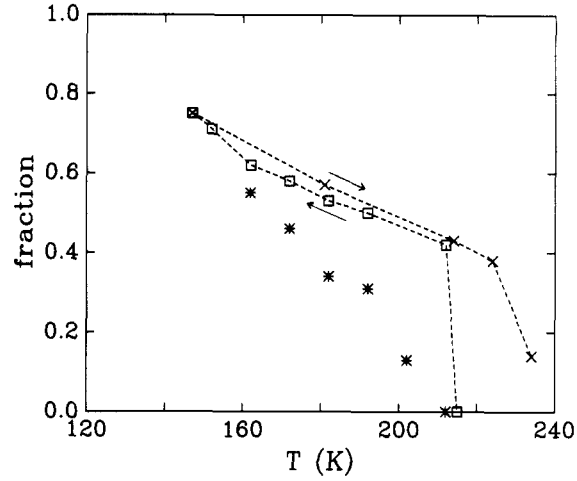

Figure 12. Fractions of solvent protons in gel samples having line widths as broad as in the pure frozen solvent. (*) iPS–*c*-D, cooling cycle; (□) iPS–*t*-D, cooling cycle; (×) iPS–*t*-D, warming cycle. Uncertainties are ±0.06. Data are based on spectra including those of Figure 11.

indicated, and spectrum N is the spectrum of the pure frozen *cis*-decalin at 192 K. At this temperature, which is 40 deg below the melting point for *cis*-decalin, its spectrum has reached the low-temperature limiting line width. Upon increasing the temperature from 192 to 215 K, the line width decreases by 15%. In contrast, the spectra (not shown) of the frozen *trans*-decalin in the region investigated, namely, from 225 to 200 K, were not temperature dependent and indistinguishable from spectrum N, Figure 11. The greater rigidity of the frozen *trans*-decalin, relative to the *cis*-decalin, is borne out by a T_1^H value (greater than 700 s) in the former at 200 K which is about 2 orders of magnitude longer than in *cis*-decalin at the same temperature.

In Figure 11N, note that the line shape of the frozen solvent is much wider than that of the PS due to the higher density of protons in the solvent. A broad base, typical of the frozen solvent line width, first appears in the gel spectra at 210 K in the iPS–*t*-D sample and at 200 K in the iPS–*c*-D sample. However, in both of these spectra, B and J, large narrower fractions remain, indicating that substantial portions of the solvent molecules have at least large-amplitude reorientational mobility. These narrower fractions diminish at lower temperatures. In Figure 12 the frozen solvent fractions are given for the two gels as a function of temperature. These fractions are determined as the ratio of the intensities possessing the frozen solvent line shape to the total solvent intensity in the samples. It is important to recognize that the spectra of Figure 11 and most of the data in Figure 12 were taken in a cooling cycle rather than a warming cycle. Therefore, undercooling effects are present.

In Figure 12, the iPS–*t*-D sample shows an abrupt increase in the amount of rigid solvent molecules at 210 K. However, only about 45% of the solvent becomes truly immobilized. Upon further cooling, more and more solvent is immobilized until about 76% of the solvent is frozen at 145 K. So even at this low temperature, 24% of the solvent molecules have not yet attained their full proton line width. However, as Figure 11H indicates, the line width of this 24% portion is quite broad. In Figure 12, data obtained by warming the iPS–*t*-D sample are also given. Only a slight hysteresis is evident between the cooling and warming cycles over the temperature range 145–215 K. There is a substantial hysteresis, however, in the 215–235 K range and it is evident that undercooling took place in

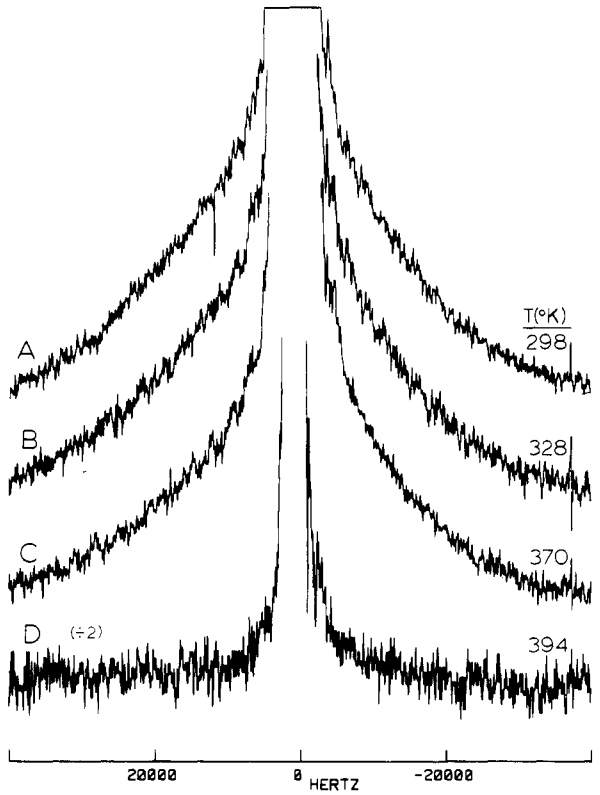

Figure 13. Broad portions of proton spectra for the iPS–*t*-D sample crystallized for 16 h at 347 K. Spectra, except for (D), are normalized to the same total intensity. The 3_1 helical crystals, which are present, have a reported melting point[1] of 393 K. These crystals show a much sharper melting behavior than the immobilized PS segments in the gels.

the cooling cycle in this temperature range. This is consistent with the DSC results to be discussed.

The freezing of the *cis*-decalin gel in Figure 12 is a much more gradual process. There is no sudden appearance of the fully broadened fraction upon cooling as there was for the iPS–*t*-D sample. This behavior is consistent with expectations based on published DSC results[7] on solvent melting for iPS–*c*-D gels, since only a very small melting endotherm is observed at this concentration. The gradual increase in frozen solvent fraction reaches about 55% at 160 K. The corresponding melting behavior was not examined in detail. Upon heating, only one temperature was examined, namely, 190 K, and for this temperature, the line shape was the same, within experimental error, as that obtained at 190 K upon cooling. Therefore, no hysteresis between 160 and 190 K seems to exist. While data at lower temperatures would offer a more complete insight into solvent freezing, we did not perform further experiments because we felt, and will presently argue, that the data in hand are sufficient to discount the existence of the postulated polymer/solvent complex.

Consistent with the DSC studies[7] of iPS–*c*-D and iPS–*t*-D gel systems, these low-temperature NMR experiments indicate that substantial amounts of solvent do not become fully rigid at the temperatures where the frozen-solvent line width first appears. Thus, a reduced melting endotherm is expected. Moreover, it is also clear that the "melting" occurs over a very wide temperature range, and in that sense, the entire melting endotherm was not captured in the reported DSC results,[8] since those scans began at 203 K. Also, the NMR results, in agreement with the DSC data, demonstrate the greater disruption of solvent freezing in iPS–*c*-D compared with iPS–*t*-D gels. Whether the proportion of nonfreezing solvent is an indication of a solvent/polymer complex will be considered in the Discussion.

Table I
T_{1D} Values[a] for Different iPS Systems

sample	preparation[b]	T_{1D}, ms
24.3% iPS–*c*-D	20 min at 253 K	0.8
24.2% iPS–*t*-D	20 min at 253 K	0.8
24.3% iPS–*c*-D	120 h at 347 K	5.5
24.2% iPS–*t*-D	16 h at 347 K	5.5
pure iPS	as originally precipitated	1.6
pure iPS	ann. 24 h at 453 K	4.5

[a] From NMR measurements at room temperature. [b] The solution samples were first heated at 454 K.

We return now to the higher temperature proton spectra. In order to illustrate the behavior of the proton line shape when iPS crystals are definitely present, we took proton spectra at various temperatures above ambient by using an iPS–*t*-D sample crystallized from solution for 24 h at 347 K. The results can be seen in Figures 8 and 13. Figure 8 indicates that the broad and narrow fractions are quite different compared with those in a gel prepared at 253 K. A much larger total broad fraction, about 0.5, is observed at room temperature, and this fraction decreases no more than 20% while the temperature is increased to 370 K (see Figure 8). A dramatic change in the line shape is observed at 394 K where the broad fraction disappears completely. This behavior is consistent with the reported 393 K melting point for chain-folded iPS single crystals in *trans*-decalin.[1] The disappearance of the broad portion occurs in a narrow interval of temperature, as expected for a regular melting of crystallites. The behavior of the narrow PS peak is complementary to that of the broad one, there being a slight increase in the narrow peak as the broad peak weakens (see Figure 8). The narrow resonance was not followed beyond 328 K since the sample begins to flow in the tube at that temperature, adversely affecting the homogeneity of the magnetic field and making integration of this line difficult. The broad lines displayed in Figure 13 are much less susceptible to sample changes of this kind; therefore, following the behavior of the broad resonances above 328 K is more informative. The results described in this paragraph are consistent with the view that at room temperature this sample contained iPS crystalline regions plus some minor gelled component which probably formed during cooling to room temperature.

From the foregoing, a clear distinction between samples prepared at 253 and 347 K is apparent. We were interested, however, in pursuing a few other experiments which might give an indication of any structural organization associated with the rigid regions of the gels. The 12_1 helical crystal structure[17] had been proposed, and even though neutron results[8] cast doubt on these structural inferences, the observation of gel melting points by DSC[7] still seemed to imply some kind of crystallinity. Therefore, we turned to the measurement of the proton dipolar relaxation time, T_{1D}. This is a relaxation time which is affected by motions in the frequency range of the dipolar interactions, i.e. the low- to mid-kilohertz range.[38] In addition, this relaxation time naturally selects the wider components of a line when the separation between the first two pulses is appropriately short (8 μs in this case). T_{1D} values also tend to be rather short so that serious complications resulting from magnetization transport (spin diffusion) are of less concern. Table I summarizes the results for different samples at ambient temperature (296 K). Decays were close to exponential. The PS/decalin T_{1D} values in Table I depend only on the temperature of preparation and not on the

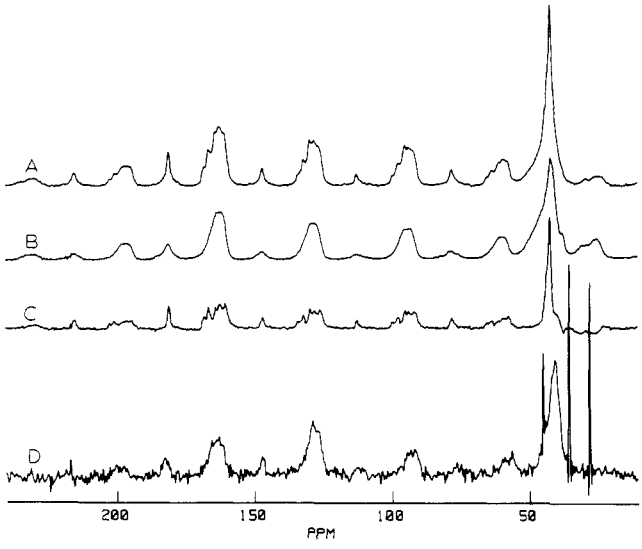

Figure 14. ^{13}C CP-MAS spectra at 296 K and a spinning frequency of 1.7 kHz: (A) semicrystalline iPS; (B) glassy iPS; (C) = (A) − 0.77(B), i.e., an approximation to the spectrum of a pure 3_1 helical crystalline preparation; (D) iPS–*t*-D gel. The sharp features in (D) are weak CP signals from the solvent carbons. Center bands of the iPS are near 42, 128, and 146 ppm; the remaining resonances are spinning side bands which mostly correspond to aromatic carbons. Fine structure in the aromatic region and the narrow aliphatic resonance in (C) are strong indications of crystalline order. CP times are all 0.7 ms.

solvent. This result points to the probable similarity of solid structures in the two solvents for a given preparation temperature. The T_{1D} for the gels is half that of the original glassy PS. Each of the samples known to contain the 3_1 helical crystalline form has a significantly longer T_{1D} than that of the gels, thus indicating stronger Fourier components of motion in the low-to-mid kilohertz frequencies in the rigid portions of the gels compared to the 3_1 helical crystals. The increased molecular mobility implied by the factor of 2 difference between the gel and glassy PS T_{1D}'s need not require that the iPS chain organization is disordered, like the glassy state. However, if the rigid phase in the gels is ordered, e.g., in a crystalline state, then the chain packing in this state appears either less perfect or less dense than in the 3_1 helical crystals, judging by the stronger Fourier components of motion. A fringed micelle structure having very limited micelle size is a possibility, although not a necessity, in this context.

^{13}C MAS Spectra. As a final effort to identify any possible crystalline structure associated with the rigid segments in the gels, we attempted a CP-MAS experiment on the iPS–*t*-D gel. The difference between ordered molecules in crystalline structures versus disordered molecules in noncrystalline structures is often reflected in these spectra by the contrast in line widths, the narrower resonances being associated with the highly ordered structures. In Figure 14 we illustrate this for two samples of pure iPS. Spectrum A is that of the annealed, semicrystalline iPS. Spectrum B is the spectrum of the mostly glassy as-precipitated iPS. Figure 14C is a linear combination of these two spectra in which a fraction of spectrum B is subtracted from spectrum A in order to accentuate the spectrum of the crystalline iPS. Note that the fine structure, barely visible in Figure 14A, is more obvious in Figure 14C. Most evident are the splittings corresponding to the five protonated aromatic carbons whose centerband region lies near 128 ppm. The aliphatic resonance near 40 ppm arising from the backbone carbons is also noticeably narrower in spectrum C than in spectrum B of Figure 14. Strong side bands, particularly for the aromatic carbons, are visible in these spectra because of the low spinning frequency employed (1.7 kHz). The low frequency was chosen in order to match the spinning conditions to those of the gel sample. A low spinning speed for the gel was considered necessary because we were not sure that the rotor seal would be liquid tight under fast rotation; further, we were concerned that the forces generated by the rotation might cause the solvent to separate from the PS although syneresis is not observed upon compression of iPS/decalin gels.[10] Even at 1.7 kHz, the gel in our rotor lost 14% of its weight over 17 h of operation. At the end of the run, the rotor was opened. A small hole was observed in the center of the sample; however, solvent and polymer still appeared well mixed. The CP-MAS spectrum of the iPS–*t*-D gel, which is shown in spectrum D, Figure 14, was accumulated during the first 2 h of spinning. Therefore, weight losses during this time are minimal and probably no larger than 2%. Unfortunately, the signal-to-noise ratio in spectrum D is less than ideal.

Two significant observations concerning this gel spectrum can be made, remembering that the intensities in the CP-MAS spectrum of the gel are strongly biased toward the more rigid molecules or residues. First, relative to the possible crystallinity of the rigid PS regions, there is no unambiguous fine structure in the protonated aromatic carbon band near 128 ppm. Ignoring signal-to-noise considerations, sharp lines resulting from an ordered structure ought to be more prominent in the spectrum of a gel with rigid, crystalline regions than in the spectrum of the pure semicrystalline iPS sample (Figure 14A), because most of the carbons in the noncrystalline residues of the gel are too mobile to cross polarize efficiently. The gel aliphatic resonance is substantially broader than in Figure 14C, moreover, its maximum is shifted about 2 ppm upfield. The lack of sharp resonances is not an absolute proof that the molecules are disordered. Molecular motion within the crystal and/or small (<5 nm) crystal dimensions can also cause line broadening. We will return to the significance of the aliphatic resonance shape in the Discussion. One clarifying comment about the aromatic resonances in the gel spectrum should be made. The aromatic center band (128 ppm) is dominant in Figure 14D, whereas the first lower side band (160 ppm) is dominant in Figure 14A,B. Normally, this would mean that there was a substantially greater mobility associated with the aromatic carbons in the gel compared to those in the glass or the crystal in contradiction to previous deductions from the carbon spectra. Actually, the most reasonable explanation for the dominant center band in the gel spectrum is that the CP-MAS spectrum includes the weak aromatic carbon resonance from those mobile residues seen at 128 ppm in the nonspinning gel CP spectrum, Figure 1A. This resonance would contribute principally to the center band and not to the side bands in the gel CP-MAS spectrum, and its contribution would be about 25% of the center band intensity. The presence of the mobile PS intensity in the aromatic center band tends to obscure any resonance fine structure. Fine structure, if present, should appear clearly in the aromatic side bands, provided the sample spinning frequency, ν_r, is not varying. Unfortunately, ν_r seems to have changed slightly during spectral acquisition judging by the broader side bands relative to the center band for the unprotonated aromatic carbon at 146 ppm. Thus, the protonated aromatic side bands are not good monitors of an ordered structure in this spectrum. The intensity ratios of side bands to each other in the gel spectrum are very similar to those in spectra A and B, Figure 14. Therefore, the gel spectrum is consistent with the general rigidity of

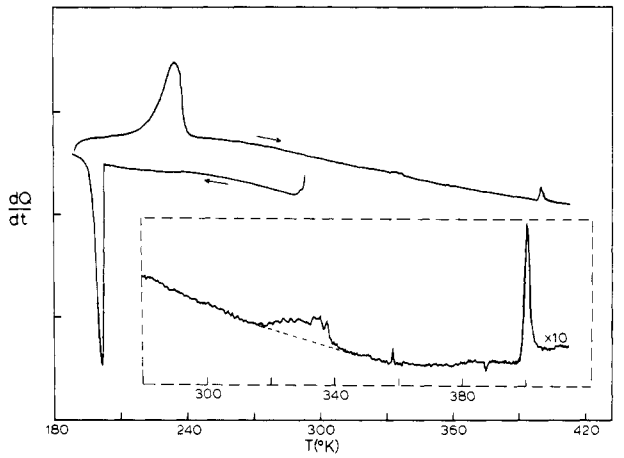

Figure 15. DSC trances of a 2-week-old iPS–*t*-D sample. A cooling run from 300 to 190 K and a warming cycle from 190 to 413 K are shown. A vertically amplified and base-line adjusted (linear correction) plot of the heating curve above the solvent melting endotherm is given in the insert. The endotherm at about 330 K relates to the gel while the sharper endotherm at 393 K indicates the dissolution of the 3_1 helical crystals present. The base line used to calculate the gel endotherm is also shown. The scan rate was 10 K/min.

the iPS segments as was inferred from nonspinning ^{13}C spectra discussed earlier.

The second comment regarding Figure 14D concerns the very sharp solvent resonances. In this spectrum, more than in spectrum C, the absence of any broad solvent resonances is obvious. The line width associated with a solvent molecule, even a mobile molecule, trapped in a PS matrix, would generally be wider than what is observed. This is particularly true for a PS crystal lattice since the aromatic rings of PS have considerable magnetic susceptibility anisotropy and this causes a broadening[31] in CP-MAS spectra. A crystalline region would be expected to possess some average orientation of the planes of the iPS rings, thus there should be significant susceptibility broadening for those solvent molecules which are trapped inside of individual crystals. Only if the solvent molecules are so mobile that they could sample crystals of several different orientations within a few ms will this broadening vanish. Given these constraints, possibilities for "solvated crystals" and/or polymer/solvent complexes become very limited.

DSC Results. DSC scans were performed on only one sample of the iPS–*t*-D gel which had been formed in a sealed tube at 253 K and refrigerated at 253 K for 2 weeks. A piece of the gel was quickly placed in an aluminum pan, sealed, and weighed. This sample was cycled in the following way: cooled to 190 K at 10 K/min, heated to 300 K at 10 K/min, cooled back to 190 K at 10 K/min, heated to 403 K at 10 K/min, immediately cooled to 253 K at 320 K/min, held for 1 h, and heated again to 403 K. Because of the limitations of the refrigerated cooling reservoir in the DSC, the cooling rate below 210 K was not controlled, i.e., became less than 10 K/min. The first and second cooling cycles to 190 K gave identical curves, indicating that the gels were not altered irreversibly by exposure to the low temperature. The second cooling and the subsequent heating thermograms are shown in Figure 15. The solvent undercooling prior to freezing is approximately the same as was seen in the pure liquid in an NMR tube. The solvent melting in the heating curve is broader than expected for a pure solvent melting. If the base line for this endotherm is taken to extend from 215 to 245 K, the heat of melting is 10.0 cal/g, in reasonable agreement with the heat of melting reported in the literature.[8] This endotherm is about 60% of that expected for the same amount of pure *trans*-decalin. The solvent melting point maximum occurs at 234 K or 9 K below the reported melting point for pure *trans*-decalin. Therefore, in the iPS–*t*-D gel there is a melting point depression, a broadening of the melting point, and a reduced endotherm compared with the pure solvent.

Figure 15 also shows small endotherms whose maxima occur at 335 and 400 K and whose integrated peaks give endotherms of 0.36 (linearly extrapolated base line from 313 to 343 K) and 0.30 cal/g. The lower portion of Figure 15 shows an expanded, amplified, and slope-adjusted section of the heating curve. The 335 K peak is in the usual range[1,7] of the gel melting temperatures and the 400 K maximum corresponds reasonably well with the melting point for the 3_1 helical crystals in *trans*-decalin;[1,7] the presence of these latter crystals demonstrates that some aging of the gel had taken place,[1,7] although we do not know what fraction of these crystals was formed during the heating. The gel melting endotherm is not sharp and is only about 8% of that expected for an identical amount of 100%-crystalline iPS having the 3_1 crystalline form.

After reaching 413 K, the sample was cooled very quickly to 253 K and held for 1 h. A repetition of the heating curve from 253 to 413 K revealed no endotherms from either the gel melting or the melting of any 3_1 helical crystals. The sample was then quickly returned to room temperature (320 K/min) and weighed; the weight was exactly the same as the starting weight (uncertainty = ±0.01 mg). A visual inspection of this sample several days later, after storage in the freezer, revealed a normal-looking gel. It is not clear why endotherms were absent from the second scan to 413 K. Similar results have been reported for iPS[38] and poly(vinyl chloride)[40] gels.

Discussion and Summary

On the Existence of a Solvent/Polymer Complex. DSC observations[8,38] seem to fit a picture of a polymer/solvent complex. Moreover, the suggestion[1,13,41] that a unique crystal structure for the iPS exists in the gels opens up the possibility that such a structure incorporates solvent. Admittedly, however, serious questions about the interpretation of the data on which such a crystal structure was inferred have been raised.[8] Just two NMR observations can be cited in possible support of a polymer/solvent complex. First, the solvent freezing data of Figures 11 and 12 agrees with the DSC findings, i.e., the presence of iPS exerts a significant influence on solvent crystallization when a gel is cooled down. Second, the increase in solvent CP signal intensities in the room temperature ^{13}C CP spectra of the gels compared to the CP intensity from a comparable amount of pure solvent is very weak further evidence for a complex. At the same time, several NMR observations make us exceedingly skeptical about a solvent/polymer complex. In fact we shall argue that such a complex does not exist. Because the data for the iPS–*t*-D sample is more complete and because both kinds of gels show the reduced solvent melting point endotherm, we will initially consider only the iPS–*t*-D system. A fundamental premise in the following argument is that if the reduction in the melting endotherm is explained in terms of a solvent/polymer complex, then in a 25% iPS–*t*-D gel, approximately half of the *trans*-decalin molecules should be complexed at the solvent freezing point.[8]

The following observations suggest the absence of a solvent/polymer complex: (a) absence of a broader decalin resonance component, above and beyond the aliphatic resonance of the iPS, in both the ^{13}C CP-MAS and nonspinning CP spectra of the gel at room temperature (this absence is especially conspicuous because the CP

process should strongly enhance those carbon resonances from solvent molecules experiencing any stronger dipolar interactions with PS molecules); (b) absence of any substantial solvent line broadening in the proton spectrum as a function of temperature, all the way down to the supercooled state at 215 K; (c) the asymptote of the intensity of the relatively broad portion of the proton line, just above the solvent freezing point, at an intensity corresponding to about 88% of the PS protons known to exist in the sample; and (d) comparable widths for the broad bases of the proton line shapes in the just-mentioned broad component and that of glassy iPS.

The only way that observations a–c above can be explained in the context of a solvent/polymer complex is that the solvent molecules in the complex are highly mobile on a 5-μs time scale and exchange with the "uncomplexed" solvent on a timescale of, at most, 1 ms. Point d above is not so easily dismissed in this context. The presence of mobile solvent should influence the line width of the backbone protons in two ways. First, the separation between chains will increase, thereby reducing the intermolecular dipolar broadening. An estimate of this line-width reduction, based on calculated and observed second moments of variously deuteriated PS samples,[32,33] is a modest 5–10% for the wide wings which arise from the backbone protons. Second, and more importantly, the presence of very mobile solvent molecules causes the intermolecular potentials for the PS chains to fluctuate rapidly. This fluctuation should result in backbone motions whose amplitudes are significantly larger than in the glass. These fast fluctuations should produce a measurable narrowing in the far wings of the spectrum. That this is not seen is further evidence that the solvent molecules are not present in significant numbers in the more rigid iPS phase.

From a thermodynamic point of view, solvent mobility within any proposed solvated-crystal lattice means that interactions between polymer and solvent are rather weak. That, coupled with the reduction in van der Waals attraction between iPS chains and the absence, in iPS, of concerns about local electrical charge neutralization, implies that the heat of formation of such a crystal would be significantly less than that of the 3_1 helical crystal. A serious question then arises why a weaker structure would form in preference to the 3_1 helical crystals which are truly stable thermodynamically at these temperatures in the presence of the solvents.

A final argument against the existence of a polymer/solvent complex comes from the low-temperature data. The low-temperature line shapes for the iPS–*t*-D system in Figure 11 do not show a uniform line broadening as the temperature is lowered for those *trans*-decalin protons which did not freeze initially. Rather, the line shape continues to exhibit both narrow and broadened features as the temperature is lowered. In Figure 12 this trend shows up as a gradual increase in the amount of "rigid" *trans*-decalin. The implication is that there is a heterogeneity of sites for the *trans*-decalin. This heterogeneity is expected if the iPS chains break up space into regions of many sizes and shapes, as will be discussed presently; however, this heterogeneity is not easily incorporated into a solvated-crystal concept, although it is, in principle, compatible with solvent inside a disordered solid.

In light of all of the foregoing points, we consider an iPS/decalin complex to be very unlikely in these gels.

Rationale for Nonfreezing Solvent. If the complex does not exist, then why is solvent freezing inhibited in the gels? In our opinion, this is mostly a physical effect, i.e., the distribution of PS chains and/or small clusters of chains at the solvent freezing point partitions space into such small domains that potential *trans*-decalin crystallites are forced into having a larger and larger surface-to-volume ratio as the concentration of iPS increases. Moreover, it is also likely that the shapes of the volumes in which the solvent crystallites can grow will be highly irregular. Both of the foregoing trends would lead to crystals which form at lower temperatures and possess a lower heat of formation (per molecule) than larger, more regularly shaped crystals. There may be some additional influence from van der Waal's attractions between the iPS chains and the solvent molecules, but the principal contribution to the melting endotherm reduction, we believe, is the lower enthalpy of fusion and the freezing point depression associated with high-surface-area solvent crystals which are forced to grow in regions through which pass enough chains, or small clusters of chains, with sufficient constraints to impose on the decalin finite crystal size and perfection. A high surface area is known to influence the melting behavior of metals,[42] and, by analogy, the dimensions over which these effects should be most noticeable are probably in the range of less than eight molecular diameters.

In the 25% iPS–*t*-D gels only about half of the pure-solvent melting endotherm is observed[8] in a DSC measurement commencing at 203 K, although it is recognized from Figure 12 that a much wider temperature range must be scanned to capture the entire melting endotherm. The data of Figure 12 support the DSC measurements in the sense that a fraction of about 0.4 is rigid in this temperature range. In light of the foregoing discussion, this raises the likelihood that there are some regions in the frozen gel where "thermodynamically large" *trans*-decalin crystals are found, i.e., those with sufficient size to have an enthalpy of fusion per molecule close to that found in pure *trans*-decalin.

Relative to the existence of some "thermodynamically large" *trans*-decalin crystals in the frozen gel, two NMR observations will be cited. Both observations lead to approximate size estimates by invoking proton spin diffusion[43] and interpreting the times for magnetization transport in terms of domain size.[44] These results are to be regarded as giving upper limits on dimensions because the frozen gels, at the temperatures indicated, contain some very mobile decalin molecules and these molecules, because of their weak dipolar interactions with their surroundings, can, depending on morphology and the extent of their dipolar coupling, become barriers to the transport of magnetization. First, the longitudinal proton relaxation time, T_1^H, in the pure solvent at 195 K, exceeds 700 s while in the frozen gel it is only 1.3 s. Supposing that the relaxation of these protons occurs by spin diffusion from the boundaries of spherical crystalline domains, upper limits for the larger crystalline dimensions are about 80 nm. We have also done some spin diffusion measurements in the iPS–*t*-D gel at 177 K starting from a state where most of the magnetization was concentrated in the protons of the larger frozen decalin crystals. On the basis of the time that it took for magnetization to move into the regions of iPS and more mobile decalin (a nonzero spin diffusion coupling exists between these regions), we inferred a reasonable population of decalin crystals whose dimensions were approximately 36 nm. Both of the foregoing results support the possibility of a population of "thermodynamically large" crystals. Again, these numbers are *upper limits* on domain sizes. How well these numbers approximate sizes depends on the largely unknown efficiency of spin diffusion in those regions of greater molecular mobility. We em-

phasize that neither of the above upper limits are relevant to the dimensions of the postulated small cavities in which solvent freezing is inhibited.

On the Nature of the Rigid Phase in the Gel. We had considerable hope that the CP-MAS ^{13}C spectrum (Figure 14D) of the iPS–*t*-D gel would give us a strong indication of ordering in the solid phase of the gel (see also the Note Added in Proof). The calling into question[8] of the limited X-ray evidence[1] for a crystal structure in the gel led us to consider the existence of ordered structures as an open issue, although infrared studies[41] on dried gels have produced evidence for partial ordering of the iPS chains. As discussed previously, the center band and side bands of the protonated aromatic carbon resonances each suffered from distortions in shape and were not useful in testing for order in the more rigid iPS phase at 296 K.

In contrast to the lack of information about ordered structures in the protonated aromatic carbon bands in Figure 14D, the nonprotonated and aliphatic carbon center bands both point to a gel structure possibly more ordered than the glass. Both of the foregoing resonances are considerably narrower than in the spectrum of the glass (Figure 14B). The shape of the aliphatic resonance in the glass is quite asymmetric and the broad downfield wing of this line is most likely due to methylene carbons. The conformational dispersion, frozen into the glass, produces a corresponding chemical shift dispersion. In PS, according to solution NMR,[45] the methylene and nonprotonated aromatic carbons have chemical shifts most sensitive to configuration; this sensitivity presumably reflects conformationally dependent chemical shifts. Thus, narrower resonances in the gel relative to the glass for these two carbons point to a smaller conformational dispersion in the gel, hence a greater order. Unfortunately, however, this is not the only explanation for these line widths. The ambiguity of interpretation arises because the gel line widths could also stem from a disordered system which undergoes some dynamical conformational averaging on a time scale shorter than, say, 0.5 ms.

Comparison of the gel CP-MAS spectrum with that of the 3_1 helical crystals (Figure 14C) reveals that particularly the aliphatic resonance is significantly wider for the gel than for the 3_1 crystals. If the gel packing were ordered, this line-width difference could point to less perfect crystals, a smaller crystallite size, or a greater motional contribution to line width[31] in the gel relative to the 3_1 crystals. Thus, the CP-MAS spectrum of the iPS–*t*-D gel supports a picture of a solid phase at ambient temperature existing somewhere between the following limits: disorder with conformational interconversion on a time scale of about 0.5 ms and order with smaller crystallite size and/or greater molecular mobility relative to the 3_1 helical crystals. The greater molecular mobility seems consistent with the shorter T_{1D}'s in the gel relative to the 3_1 crystals. It must be remembered, however, that this "greater mobility" is a relative term and, to maintain consistency with the nonspinning ^{13}C and proton line shapes, must still be restricted; e.g., if large amplitudes are involved (e.g. conformational interconversion) then frequencies must be restricted to below a few kilohertz.

A final point about the gel spectrum (Figure 14D) is that the aliphatic resonance maximum, which is associated with the methine resonance,[45,46] is shifted 1.5–2.0 ppm upfield from that of the glass (Figure 14B) or the semicrystalline preparation (Figure 14A). There is a question whether this shift is real since all spectra of Figure 14 were run without an internal chemical shift standard. Since spectra A, B, and D were run consecutively, the shift scale should be very reproducible; however, the rotor material for the gel was different from that containing the pure PS samples. This could have caused a shift of spectrum D relative to spectra A–C. The chemical shift scale was chosen so that the *trans*-decalin resonances in Figure 14D would coincide with the published shifts[47] of *trans*-decalin. Using this scale, one obtains shifts for the aliphatic and the nonprotonated aromatic carbons in Figure 14C which are about 0.6 ppm smaller than the corrected,[48] published values[46] for crystalline iPS. In other words, the alignment of the spectra in Figure 14 is probably accurate within 0.8 ppm.

Of special significance in the gel spectrum is that the chemical shift difference, separating the resonance maxima of the nonprotonated aromatic and aliphatic carbons, is 1.5–2.0 ppm greater in Figure 14D than in any of the other three spectra in Figure 14. Since chemical shift differences within the same molecule cannot be attributed to bulk magnetic susceptibility effects,[31] we conclude that this unique chemical shift difference points to a structure different, on average, from the glass and different from the 3_1 helix. While the simultaneous presence of resonance intensity from both rigid and more mobile iPS segments introduces some uncertainty into the determination of the resonance positions, the intensity arising from the more mobile segments is insufficient to adequately explain this effect. The uncertainty in spectral alignment introduces an uncertainty as to whether the foregoing effect is due entirely to an upfield shift of the methine resonance or, at the other extreme, whether both resonances shift equally but in opposite directions. Intuition might suggest that the largest shift ought to occur in the more conformationally sensitive carbon, namely, the nonprotonated aromatic carbon. This is not borne out.

Based on the foregoing unique chemical shift difference in the gel spectrum and the narrower (relative to the glassy state of iPS) resonance profiles of the aliphatic and nonprotonated aromatic carbons in the gel, we conclude that it is likely, but not proven, that at 296 K the gel phase is more ordered than the glass, although greater order need not imply crystallinity.

The Meaning of the Liquidlike Fraction. Figures 7 and 8 show that the sum of the "liquidlike" and "relatively rigid" fractions of the iPS resonance does not add up to unity for most temperatures, i.e., some segments have intermediate mobility. We now ask the question whether the existence of and the temperature dependence of the liquidlike fraction provide any insight into gel structure. The following are some very qualitative comments about the liquidlike line.

In order to identify the aromatic proton resonance as liquidlike and distinguish it from that of the solvent, we assume the natural linewidth must be 400 Hz or less. The second assumption is that all chain fragments giving rise to the mobile fraction are fixed at both ends. This approximation should be reasonable since M_n is large for this iPS. Then what conditions must prevail in order that a chain fragment will possess such a narrow resonance? According to Cohen-Addad,[49] the line width, lw, of a flexible chain segment, fixed at both ends, is given by

$$\mathrm{lw}(\beta) = \mathrm{LW}(\beta)/R_2 \qquad (1)$$

where β is the angle between the end-to-end vector of the segment and the static field, LW is the line width in an isolated, rigid chain oriented at the angle β, and R is the contour length divided by the end-to-end distance of the segment. Equation 1 predicts a dispersion of line widths, even for a fixed R, when distributions of β are present. If we assume for simplicity that $\mathrm{LW}(\beta)$ varies as $(3\cos^2\beta - 1)$, that the gel is unoriented, that the average, rigid-lattice

line width for the aromatic protons on an isolated PS chain is 24 kHz,[32,33] and that all chain segments have the same R at any temperature, then, from the data of Figure 8 for the iPS–t-D gel, R is estimated to be 7.8, 7.0, 5.3, 4.2, and 2.1 at 303, 296, 284, 270, and 255 K, respectively. These numbers are calculated to be consistent, not only with the rigid and liquidlike fractions, but also with the remaining PS resonance intensity not belonging to these fractions. If some allowance for aromatic ring rotation is included, then the R values decrease by about 16% at each temperature. These numbers should be taken as approximate, and the smaller numbers should be viewed as lower limits since it is more difficult to identify that portion of a line having line widths less than, say, 400 HZ when the remainder of the line is becoming very broad. It is reasonable to conclude from this approximate calculation that the segments in solution are getting shorter as the temperature of the gel is lowered.

Ruminations about Gel Structure in Light of the NMR Observations. The following speculative discussion about iPS–decalin gel structure is written in an attempt to reconcile several kinds of observations reported in this paper and elsewhere.

An important NMR result is that the fraction of rigid phase decreases continuously with increasing temperature over a range of about 100 K, from the temperature of the supercooled solvent to the reported gel melting temperature. Concurrent with this decrease is an increase in a liquidlike fraction. Moreover, both fractions are reversible, at least in the region from ambient temperature down to the solvent freezing temperature. Therefore, whatever structure we argue for must possess this reversibility.

In contrast to this reversible behavior, there is the recognition that gel melting endotherms appear at temperatures higher than maximum gel formation temperatures.[5,7,38] In this sense, the gels display a considerable hysteresis, and any model must also account for this lack of reversibility.

Most likely the formation of the gel structure at 253 K in the iPS–t-D or iPS–c-D systems initially involves some liquid–liquid phase separation.[7,12,50] There is also a possibility that crystallization, even chain-folded crystallization,[5] occurs during this phase separation via some nucleation process. Such crystallization can explain the difference between onset temperatures of gel formation and gel melting temperatures as well as the higher onset temperatures for gel formation in iPS versus that in atactic PS. In the liquid–liquid phase separation, two phases develop, one more concentrated in iPS than the original solution and one less concentrated. Presumably, the first nucleation (condensation) events take place preferentially in the concentrated phase. It follows that the "scaffolding" of solid iPS forms in these regions. Even in these more concentrated regions, the process of condensation involves the gathering of chain segments from a larger volume of solution, and, if several nuclei are forming simultaneously, it is not clear that the solid regions formed should, themselves, agglomerate to form a dense solid structure which excludes solvent from all interior regions. Rather, the scaffolding formed from the more concentrated iPS phase may be built from more loosely aggregated, relatively small, solid regions. The surface area associated with such an open structure would also be larger than if the scaffolding members were dense in iPS. Depending on the average contour length of chain segments in contact with the solvent, a high surface area for the scaffolding could be implied, for example, at 280 K in 25% iPS–t-D where about 50% of the segments are in contact with the solvent according to Figure 8. Also, relative to the solvent freezing behavior, it would be easy to imagine how, within such an open scaffolding at lower temperatures, the iPS chains could partition this space into very small regions so that solvent crystallization would be inhibited. If this picture has merit, in the iPS–t-D system the larger *trans*-decalin crystallites would likely form in those regions initially reduced in iPS concentration by the phase separation.

If we follow the line of reasoning of phase separation followed by the formation of nuclei having ordered structures as the first stage of condensation, then what kind of a structure develops at the latter stages of condensation? We assume, with the high molecular weights of iPS present in the samples studied herein, that following the nucleation stage each molecule participates in at least two nuclei and that most segments remaining in solution are fixed at both ends. Then the later stages of condensation mostly involve the "reeling in" of these chains onto the existing sites of nucleation. If further nucleation of ordered structures was important, then one would expect significant hysteresis in curves like Figures 7 and 8. This is not observed in the range from 296 K to the solvent freezing points. Thermodynamically, it makes sense that this continuing process of condensation favors ordered over disordered structures; however, the constraints imposed by entanglements and the attachment of the chains at two ends may prevent the growth of large ordered structures. Therefore, to observe (at 296 K where 25% of the chain segments are condensed) that these condensed segments are more ordered than the glass seems reasonable; to recognize that they also show less order and/or more mobility than the 3_1 helical crystals is also reasonable because the ordered domains formed are probably small, particularly those formed after the original nucleation.

As a result of the original liquid–liquid phase separation there are solvent-rich regions. In such regions few if any iPS nuclei are expected to form; however, these regions probably have a nonzero concentration of iPS as the following observations imply. First, in the 25% iPS–c-D there is no space, devoid of iPS, large enough to allow *cis*-decalin crystals to grow at the usual freezing temperature for pure *cis*-decalin. Second, these gels show very little syneresis[10] and this is difficult to understand if one has a bicontinuous scaffolding with characteristic distances of the order of tenths of micrometers.[7,11] If the gaps between the scaffolding had no iPS chains, then syneresis would be expected. With respect to the characteristic distances between elements of the scaffolding, to our knowledge there are no distances reported in the literature for the 25% gels studied herein; the tenths of a micrometer distances[7] are related to gels formed at lower concentrations and in different solvents.[11] At the higher concentrations, these characteristic distances may be significantly reduced. We recognize that our explanation for the inhibition of solvent freezing in these gels relates to these characteristic distances in the following way: the density of iPS chains in the solvent-rich regions must, of physical necessity, be a diminishing function of the distance from the surface of the solid iPS domains. Thus, if the characteristic distance of separation of the scaffolding elements becomes too large, the ability to inhibit crystallization, especially in the interior of the solvent-rich regions, would be correspondingly diminished.

We also offer the following speculations regarding the stronger influence of the iPS chains in suppressing crystallization in *cis*- versus *trans*-decalin gels. Pure *cis*-decalin has a heat of fusion about two-thirds that of *trans*-decalin.[8] Therefore, a *cis*-decalin molecule is more weakly bound

in its crystal than is the *trans*-decalin molecule in its crystal. It follows that for a very small, forming crystallite, the deposition of a *cis*-decalin molecule is not as energetically favored as for the *trans*-decalin case. Therefore, at any given temperature the minimum size of a stable crystal of *cis*-decalin may be larger than that of *trans*-decalin; thus a given distribution of iPS chains could inhibit solvent crystal formation more effectively in *cis*- versus *trans*-decalin gels. If this picture is correct, however, then in order to get a near-total suppression of solvent crystallization at the solvent freezing point in the 25% iPS–*c*-D gel[8] (see also Figure 12), it would seem that regions dilute in iPS (which result, say, from initial liquid–liquid phase separation) should not, in contrast to iPS–*t*-D gels, be so dilute in iPS that "thermodynamically large" crystals can form. This, in turn, suggests one or a combination of the following: (a) the dilute-phase concentration of iPS in the cis gels is higher than that of the trans gels, (b) *cis*-decalin has a stronger affinity for iPS than has *trans*-decalin, and (c) the characteristic scale of the iPS scaffolding is smaller in the *cis*- versus the *trans*-decalin gels. The latter possibility arises from the recognition that the density of iPS chains in the solvent-rich regions is a diminishing function of distance as one moves away from the regions of condensed iPS.

In Figures 7 and 8 there is no indication of any major rearrangements occurring in the range from 253 to 296 K. Yet, the clear/turbid transition[7] lies in this range. The NMR results suggest that the clear/turbid transition in these gels is likely to be that point where the scaffolding becomes thick enough and the contrast in the refractive indices between the solid and the solvent-rich regions becomes high enough to scatter light. The dimensions of the scaffolding may well be on the order of the wavelength of light at all temperatures where the gel exists. This explanation would not predict a sudden appearance of turbidity, rather a more gradual increase in light scattering would be expected.

Finally, it is interesting to us that the iPS–*c*-D gel formed by slowly cooling a solution from 304 to 295 K overnight in a Dewar filled with water gave rigid and mobile fractions, at ambient temperature, which are experimentally indistinguishable from the fractions characterizing gels formed by quenching to 253 K. If liquid–liquid phase separation is the first step in gel formation, it is likely that the distance scales for these two preparations are quite different. Yet their fractions are the same. In principle, this result can be achieved by simply scaling all dimensions including the thickness of the scaffold elements; the only requirement in the simple scaling picture is that the lengths of the fragments in solution must also scale. If all dimensions were simply scaled, solvent freezing behavior could be altered; such an inquiry, along with many others, remains for future work.

Note Added in Proof. Recent CP-MAS spectra of a 25% iPS–*t*-D gel have been obtained at ambient temperature, without appreciable solvent loss, with a more stable spinning speed, and with improved signal-to-noise. All features claimed to be associated with the CP-MAS spectrum of the gel in this paper were corroborated. Additionally, the aromatic sidebands showed weak, but definite, fine structure patterns which did not fully agree with the fine structure patterns characterizing the 3_1 helical crystals. (Subsequent DSC analysis of this sample at a scan rate of 5 °C/min indicated that an upper limit of only 2% of the iPS segments could be identified with 3_1 helical crystals; this amount is too small to explain the intensity of the fine structure observed.) The weak shoulder, identified with the iPS backbone carbons, was also visible at 43.5 ppm, right beneath the most downfield line of the *trans*-decalin. The above provides further support that the solidlike iPS segments in the iPS–*t*-D gel at room temperature are, on average, more ordered than the glass. The fine structure in the aromatic sidebands seems to support the idea that a minority (ca. 20%) of the more rigid iPS segments are in a state of significant order, with a majority disordered. On the other hand, the pervasive change in the position of the aliphatic resonance suggests that a majority of the more rigid iPS segments are participating in an environment distinct from either the glass or the 3_1 helical crystals.

We have also recently become aware that the rationale for solvent freezing point depression has been put forth by Kuhn et al. (Kuhn, W.; Peterli, E.; Mayer, H. *J. Polym. Sci.* **1955**, *16*, 539). This explanation is also controversial; it has been challenged, for example, by Boonstra et al. (Boonstra, B. B.; Heckman, F. A.; Taylor G. L. *J. Appl. Polym. Sci.* **1968**, *12*, 223) and Oikawa and Murakami (Oikawa, H.; Murakami K. *Polymer* **1986**, *27*, 1563).

Acknowledgment. We thank Drs. C. C. Han, E. A. Di Marzio, and C. M. Guttman for helpful discussions. Appreciation is also expressed to the Research Council of Spain (CSIC) for the award of a research grant which supported one of us (E.P.) while conducting this work at the National Bureau of Standards.

Registry No. iPS, 25086-18-4; *cis*-decalin, 493-01-6; *trans*-decalin, 493-02-7.

References and Notes

(1) Girolamo, M.; Keller, A.; Miyasaka, K.; Overbergh, N. *J. Polym. Sci., Polym. Phys. Ed.* **1976**, *14*, 39.
(2) Tan, H. M.; Chang, B. H.; Baer, E.; Hiltner, A. *Eur. Polym. J.* **1983**, *19*, 1021.
(3) Tan, H. M.; Moet, A.; Hiltner, A.; Baer, E. *Macromolecules* **1983**, *16*, 28.
(4) Boyer, R. F.; Baer, E.; Hiltner, A. *Macromolecules* **1985**, *18*, 427.
(5) Domszy, R. C.; Alamo, R.; Edwards, C. O.; Mandelkern, L. *Macromolecules* **1986**, *19*, 310.
(6) Guenet, J.-M.; Willmott, N. F. F.; Ellsmore, P. A. *Polym. Commun.* **1983**, *24*, 230.
(7) Guenet, J.-M.; Lotz, B.; Wittmann, J.-C.; *Macromolecules* **1985**, *18*, 420.
(8) Guenet, J.-M. *Macromolecules* **1986**, *19*, 1961.
(9) Gan, J. Y. S.; Francois, J.; Guenet, J.-M. *Macromolecules* **1986**, *19*, 173.
(10) Guenet, J.-M.; McKenna, G. B. *J. Polym. Sci., Polym. Phys. Ed.* **1986**, *24*, 2499.
(11) Aubert, J. H.; Clough, R. L. *Polymer* **1985**, *26*, 2047.
(12) Wellinghoff, S.; Shaw, J.; Baer, E. *Macromolecules* **1979**, *12*, 932.
(13) Sundararajan, P. R.; Tyrer, N. J.; Bluhm, T. L. *Macromolecules* **1982**, *15*, 286.
(14) Blum, F. D.; Nagara, B. N. *Polym. Prepr. (Am. Chem. Soc., Div. Polym. Chem.)* **1986**, *27*(1), 211.
(15) Atkins, E. D. T.; Isaac, D. H.; Keller, A. *J. Polym. Sci., Polym. Phys. Ed.* **1980**, *18*, 71.
(16) Aubert, J. H. *Polym. Prepr. (Am. Chem. Soc., Div. Polym. Chem.)* Denver, CO, April, 1987.
(17) Natta, G.; Corradini, P.; Bassi, I. W. *Nuovo Cimento Suppl.* **1968**, *15*(1), 68.
(18) Walters, A. T. *J. Polym. Sci.* **1954**, *13*, 207.
(19) Leharne, S. A.; Park, G. S. *Eur. Polym. J.* **1983**, *19*, 1147.
(20) Andrew, E. R. *Progr. Nucl. Magn. Reson. Spectrosc.* **1972**, *8*, 1.
(21) Lowe, I. J. *Phys. Rev. Lett.* **1959**, *2*, 85.
(22) Schaefer, J.; Stejskal, E. O.; Buchdahl, R. *Macromolecules* **1975**, *8*, 291.
(23) Garroway, A. N.; Moniz, W. B.; Resing, H. A. *Prepr. Div. Org. Coatings Plastics Chem.* **1976**, *36*, 133.
(24) Certain commercial companies are named in order to specify adequately the experimental procedure. This in no way implies endorsement or recommendation by NBS.
(25) Pines, A.; Gibby, M. G.; Waugh, J. S. *J. Chem. Phys.* **1973**, *59*, 569.

(26) Jeener, J.; Broekaert, P. *Phys. Rev.* **1967**, *157*, 232.
(27) Van Geet, A. L. *Anal. Chem.* **1970**, *42*, 679.
(28) Mehring, M. *NMR: Basic Principles and Progress*; Springer-Verlag: Berlin, 1976; Vol. 11, Chapter V.
(29) Bertrand, R. D.; Moniz, W. B.; Garroway, A. N.; Chingas, G. C. *J. Am. Chem. Soc.* **1978**, *100*, 5227.
(30) Chingas, G. C.; Garroway, A. N.; Bertrand, R. D.; Moniz, W. B. *J. Chem. Phys.* **1981**, *74*, 127.
(31) VanderHart, D. L.; Earl, W. L.; Garroway, A. N. *J. Magn. Reson.* **1981**, *44*, 361.
(32) Odajima, A.; Sauer, J. A.; Woodward, A. E. *J. Polym. Sci.* **1962**, *57*, 107.
(33) Willenberg, B.; Sillescu, H. *Makromol. Chem.* **1977**, *178*, 2401.
(34) Lindner, P.; Rossler, E.; Sillescu, H. *Makromol. Chem.* **1981**, *182*, 3653.
(35) Spiess, H. W. *Colloid Polym. Sci.* **1983**, *261*, 193.
(36) Bergmann, K. *Kolloid Z. Polym.* **1973**, *251*, 962.
(37) Olf, H. G.; Peterlin, A. *Kolloid Z. Z. Polym.* **1967**, *215*, 97.
(38) Guenet, J. M.; McKenna, G. B. *Macromolecules*, in press.
(39) Goldman, M. *Spin Temperature and Nuclear Magnetic Resonance in Solids*; Oxford University Press: London, 1970; Chapter 3.
(40) Yang, Y. C.; Geil, P. H. *J. Macromol. Sci.* **1983**, *B22*(3), 463.
(41) Painter, P. C.; Kessler, R. E.; Snyder, R. W. *J. Polym. Sci., Polym. Phys. Ed.* **1980**, *18*, 723.
(42) Swalin, R. A. *Thermodynamics of Solids*; Wiley: New York, 1972, p 180 ff.
(43) Abragam, A. *Principles of Nuclear Magnetism*; Oxford University Press: London, 1961; Chapter V.
(44) Packer, K. J.; Pope, J. M.; Yeung, R. R.; Cudby, M. E. A. *J. Polym. Sci., Polym. Phys. Ed.* **1984**, *22*, 589.
(45) Randall, J. C. *J. Polym. Sci., Polym. Phys. Ed.* **1975**, *13*, 889.
(46) Earl, W. L.; VanderHart, D. L. *J. Magn. Reson.* **1982**, *48*, 35.
(47) *Atlas of Carbon-13 NMR Data*; Breitmaier, E., Haas, G., Voelter, W., Eds.; Heyden: London, 1979.
(48) VanderHart, D. L. *J. Chem. Phys.* **1986**, *84*, 1196.
(49) Cohen-Addad, J. P. In *Structure and Dynamics of Molecular Systems-II*; Daudel, R., Ed.; Reidel: Dordrecht, Holland, 1986; p 155 ff.
(50) Cahn, J. W. *J. Am. Ceram. Soc.* **1969**, *52*, 118.

Microdomain Characterization of Styrene–Imidazole Copolymers

R. C. Sutton, L. Thai, J. M. Hewitt, C. L. Voycheck, and J. S. Tan*

Research Laboratories, Eastman Kodak Company, Rochester, New York 14650. *Received August 21, 1987*

ABSTRACT: The microstructures of several copolymers of styrene and *N*-vinylimidazole in dilute solutions and cast films were investigated by fluorescence, ^{13}C NMR, light scattering, viscosity, and electron microscopy. Random sequence distribution of the copolymers was characterized by ^{13}C NMR. Despite such random distribution of the styrene and imidazole groups along the chain, phase separation of the hydrophobic styrene and the hydrophilic imidazole domains is suggested by several experimental findings. Smaller hydrodynamic volumes of such styrene–imidazole copolymers in polar solvents were measured compared to those for the homopolymer, poly(*N*-vinylimidazole), at comparable molecular weights. This is attributed to the aggregation of styrene residues in the polar environment. A sharp conformational change of these copolymers in aqueous media from a supercoiled dispersion to a water-soluble extended coil can be induced by protonation of the imidazole moiety. Local aggregation of the styrene groups and electrostatic repulsion of the protonated imidazolium groups are the causes for such a transition. The styrene aggregation was further characterized by the styrene emission spectra of the copolymers. The excimer-to-monomer peak ratio of the intrinsic styrene chromophore varies with copolymer composition, solvent, and pH, suggesting the effect of long-range interaction on styrene excimer formation. Separation between the styrene and imidazole domains was further verified by the absence of energy transfer from the styrene chromophore as the donor to an acceptor probe, 1-pyrenesulfonic acid, complexed at the imidazole site. Such phase separation is manifested in films cast on water from organic solutions of the copolymers. These results suggest that the hydrophobic/hydrophilic random copolymers behave as polymeric surfactants characterized by a micellelike structure in an aqueous environment.

Introduction

For various applications of polymers, copolymers are frequently employed to achieve optimal functionalities of the component comonomers. Random copolymers of styrene and *N*-vinylimidazole as shown by the following formula are such examples.

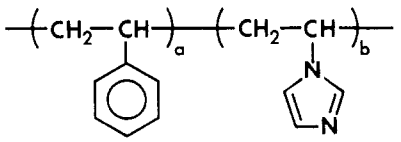

The hydrophilic imidazole moiety is used to provide the reactive sites for metal ion complexation, dye binding, or oxygen quenching; the hydrophobic styrene moiety is used to enhance the binding strength of dye molecules and other desired physical properties in the film. These properties are greatly affected by the microstructures of the copolymers in solutions and solid states. The objective of the present work is to characterize the microstructures of such systems by using various microscopic and macroscopic techniques. Correlation between polymer structures and interactions with dye molecules will be reported in a separate paper.[1]

While phase separation is a common phenomenon in block and graft copolymers, less is known about random copolymers. Because of the diametric solubility behavior of the component styrene and imidazole moieties, polymer conformation and the morphology of cast film can be manipulated by the nature of the solvent. In the present study, several experimental facts are provided to support the existence of styrene-phase formation.

In an aqueous medium, formation of a micellelike dispersion is expected, consisting of the water-insoluble styrene core and the water-soluble imidazole groups distributed on the surface of the dispersion. Such a process is driven by an entropic gain associated with the migration of the hydrophobic styrene groups from an aqueous environment to the interior of the polymer dispersion. The flexibility of the backbone chain is required for this segmental reorientation. Such micellelike structures can be altered by solvent or pH changes as depicted in Figure 1. In an acidic medium, the polymer coil is extended and soluble in water (structure a), resulting from protonation of the imidazole groups. An increase in pH above 4.0

0024-9297/88/2221-2432$01.50/0